Data Visualization for Statistical Analysis and Discovery in Container Surface Characterization at the Nano-Scale and Micro-Scale

James George Wendelberger* and Paul Herrick Smith†

*Statistical Sciences (of Computer, Computational, and Statistical Sciences Division)
†Strategic Science & Engineering (of Plutonium Science and Manufacturing Directorate)
Los Alamos National Laboratory, Los Alamos, New Mexico, USA
E-mail: JGW@LANL.GOV, SMITHP@LANL.GOV

***Abstract*—Visualization is used for stainless steel container wall and lid cross section characterization. Two specific types of containers are examined: 3013 and SAVY. The container wall examined is from a sample of the inner container of a 3013 container. The inner lid cross section examined is from a SAVY container. Laser confocal microscope data and photographic data are used to determine features of the surfaces. The surface features are then characterized by various feature statistics, such as, maximum depth, area, eccentricity, and others. The purpose of this pilot study is to demonstrate the effectiveness of using the methodology to detect potential corrosion events on the inner container surfaces. The features are used to quantify these corrosion events. An automatic image analysis system uses this methodology to classify images for possible further human analysis by flagging possible corrosion events. A manual image analysis methodology is used to determine the amount of MnS on the SAVY container lid cross section. Visualization is an integral component of the analysis methodology.**

***Index Terms*—laser confocal microscope, pits, cracks, stress corrosion cracking (SCC), surface corrosion, container integrity, characterization**

I. Introduction

The contribution of this work is to demonstrate how to employ innovative analyses, state-of-the-art image analysis methods, and visualization methodology in the evaluation of container surfaces to aid in the human inspection of the container and to detect surface aspects of interest. Specifically, in this study, these surface aspects are:

- Identification of potential pitting, potential cracking, or potential general surface corrosion and
- Amount of MnS on the surface of a container lid cross section.

Two different surface analysis examples are provided: one example for identification of potential pitting, potential cracking or potential general surface corrosion using laser microscope data and a second example determining the amount of MnS on container surfaces. The tasks of the visualization and data analysis is to identify corrosion and quantify MnS in these examples.

LEVIA'18: Leipzig Symposium on Visualization in Applications 2018

The motivation of this analysis and discovery is in the application area of hazardous material container corrosion quantification. The hazardous material may be compounds of Uranium and or Plutonium [1]. These materials have a tendency to corrode the stainless steel containers in which they are held. There are various container types that have evolved over the years. These types include Hagan, 3013, and SAVY containers [2], [3], [4], [5], [6], and [7]. In this study we look at examples from 3013 and SAVY container inner surfaces. The inner surfaces are those that corrode due to the material and are of most concern. These containers are designed to meet certain specifications. In this paper in addition to corrosion analysis, the quantification of the inner surface samples is used to determine whether or not the containers meet these specifications.

Consider the surface depicted in Fig. 1. This image is composed of the red, green, and blue (RGB) channels of the optical data from a Keyence Laser Confocal Microscope (LCM). The RGB channel data is not encoded by the authors but rather the RGB optical data is exported, as is, by the microscope within a ".vk4" formatted file. The image is a magnification of the optical appearance of the inner surface of an inner 3013 container. Although, coded in color, the image appears rather monochrome or bland, exhibiting a hint of blue-green and light tan colors, along with the grey and black features. It is desired to analyze the optical and other related data, described below, to determine where potential pitting, stress corrosion cracking (SCC), or surface corrosion may occur. Related data produced by the microscope are surface depth & height, laser intensity, and laser optical measurements. Optical data is a straight visual coding of the sample and laser optical data modifies the optical data using the laser measurement of the microscope, see [20] for details.

Older, non 3013 and non SAVY, containers have failed for various reasons, and 15 instances of container failure have occurred between 1969 and 1999 [1]. To avoid failure in the 3013 containers the 3013 standard states: "Storage containers that meet these criteria should maintain their integrity (i.e., should not require repackaging) for a minimum of 50 years" [3], and the storage plan should "assure that 3013 containers

can be safely stored for up to 50 years". The standard also points out "Stress corrosion cracking has been identified as being the greatest threat to 3013 container integrity." The solutions presented here are meant to monitor the corrosion progress on containers in light of the standard requirements.

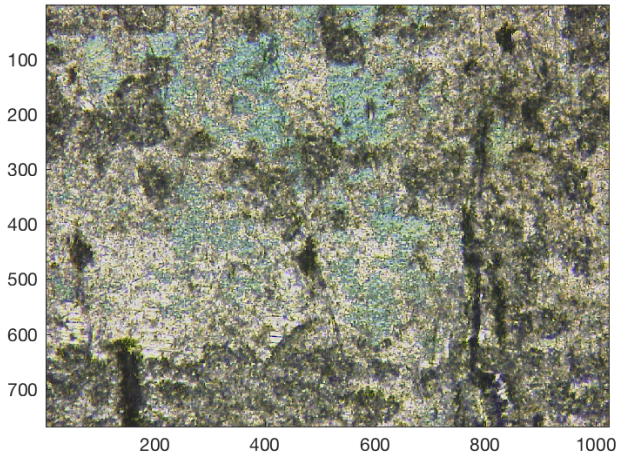

Fig. 1. Example of RGB optical data, 768 rows by 1024 columns image, from a confocal microscope ".vk4" data file. Axes represent row (vertical) and column (horizontal) pixel numbers. Pixel width and height are both 695 nm, [8].

The surface depicted in the photograph in Fig. 2 is a cross section of the lid of a SAVY container, [9]. A stringer is a very narrow "tunnel" through the container lid identified as a dark spot on an image comprising MnS. The resolution of the image and small size of the stringers make it very hard to see the stringers in the image. Fig. 3 is a zoomed-in area of Fig. 2 showing more of the stringers as dark areas and making the structure of the stainless steel more visible as patchy silvery areas. The problem is to determine the area and area ratio (stringer area to total image area) of the manganese sulfide (MnS) "stringers" in the image. The stringers are represented by the dark areas in the photograph. The bright white area in the dark feature in the lower left of Fig. 2, see zoom of area in Fig. 4, is believed to be polishing material in a void, an artifact of the sample preparation. The area and area ratio is needed to determine if the sulfur content of the SAVY lid is within the required specification [4].

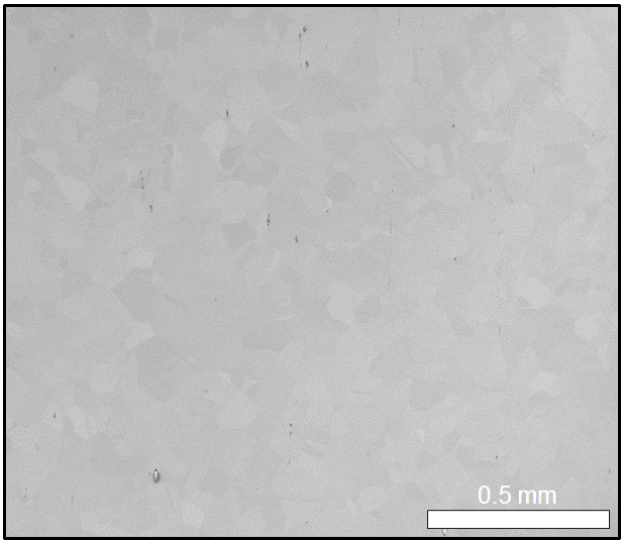

Fig. 2. SAVY container photographic image. Dark areas are indicative of stringers containing MnS, [9]. Inside the frame of this image are 525 rows and 606 columns of pixels. One pixel width and height are both 2.8 μm, [9].

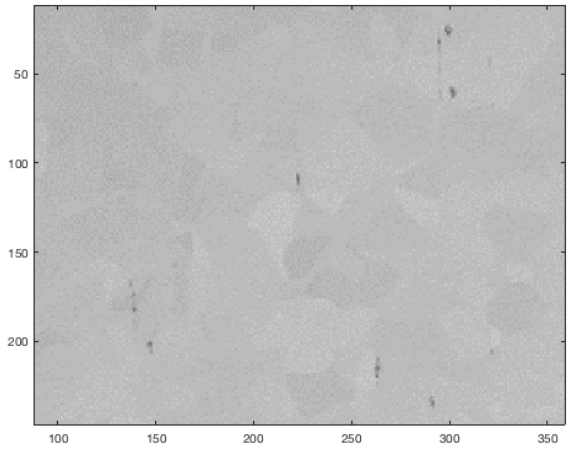

Fig. 3. SAVY container zoom in of photographic image in Fig. 2. Axes values reflect rows and columns of the zoom area.

II. Background

The primary purpose of this work is to detect potential pits, cracks, surface corrosion, and other surface aspects. There are various works describing the nature and growth of corrosion features, see for example, [10], [11], [12], [13], [14], [15], [16], [17], and [18]. The nature of this work identify surface features and to give descriptive statistics of the identified features. Identifying a feature is one critical component of this research. A feature is anything on the surface that is not the horizontal plane representing a "flat" mean surface level. Features may be formed on a height surface and thus represent depressions in the surface or possibly debris above the surface. Features formed on intensity or optical surfaces may simply represent reflectance differences or discolorations in the average intensity or optical surface. The descriptive statistics for features may be used to accomplish the goals of the analyses, such as, defining maximum pit depth, identifying stress corrosion cracking, or quantifying the amount of MnS. The techniques developed originally for corrosion analysis support other applications, for example the stringer analysis for determining the area of MnS on a cross section of a SAVY container lid. The identification of features allows for the detection of potential pits, cracks, surface corrosion, and other surface aspects, and to quantify the desired aspects in order to answer the research task.

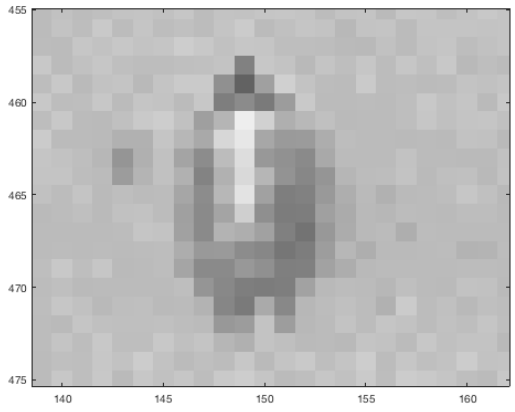

Fig. 4. Zoom of feature in lower left of Fig. 2. Rows and columns of Fig. 2 are on the axes.

A. Laser Confocal Microscope (LCM) data

The container is sectioned and the inner container surface is interrogated with a laser confocal microscope. The optical data displayed in Fig. 1 has an integer, in the range (0,255), triple corresponding to the red, green, and blue color channels for each pixel in the image representing the color of the surface as measured by the microscope. The microscope records the information about the state of the microscope and the resulting measurements in a file with Keyence, [20], format ".vk4". How to extract this information with MATLAB software is described and provided in [19]. For the purpose of this document the data consist of four images, typically, these images are of size 768 by 1024 pixels. The header contains the information about the size of a pixel in microns. The images are: height, intensity, optical, and laser optical. The height and intensity image data values are both univariate integers per pixel and the optical and laser optical image data values are RGB color images with three color values (integer from 0 to 255) per pixel. For more detail on the data one would need to contact the microscope vendor Keyence, [20].

The detailed analysis of the depth & height data is described in [21]. The depth & height data consists of a positive integer for each pixel in a 768 by 1024 matrix. Normalizing this data by dividing by the largest observed integer in the matrix yields the image in Fig. 5. A general trend of the depth & height data can be seen in Fig. 5. The upper right corner tends to be high and the lower left corner low. This is a consequence of the sample of the container that is put in the microscope being either curved itself and or being placed upon the microscope stage in a slightly non-horizontal way. This data discovery leads to removal of this "tilt" for further analysis purposes.

The removal of this "tilt" is called background removal, [21]. The background of the image is estimated by a very low frequency function fit to the depth & height data, [8]. The function fit is accomplished with the subroutine SMOOTHN [22], [23], [24], in MATLAB version 2017a using a fixed smoothing parameter of 1,000,000. To make for a more rapid analysis in the discovery phase of this analysis, the smoothing parameter has been fixed at a user specified value, here 1,000,000. It is envisioned that this parameter will be estimated for each image, up to 6,000 images, in the automated analysis system. This background is removed from the original data by subtracting the background from the data at each pixel in the matrix or image. The resulting background removed depth & height data is portrayed in Fig. 6.

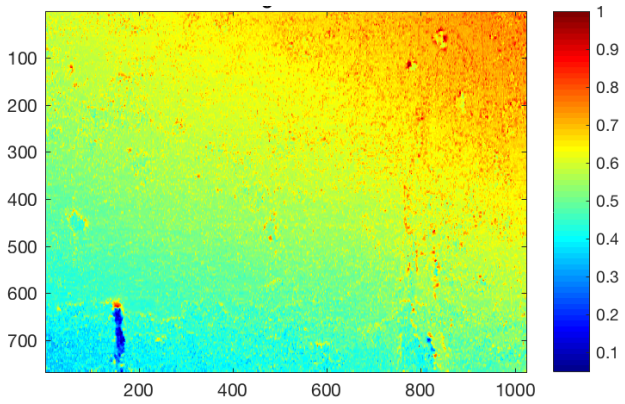

Fig. 5. Example of depth & height data, 768 rows by 1024 columns image, from a confocal microscope ".vk4" data file. Axes represent row (vertical) and column (horizontal) pixel numbers. Pixel width and height are both 690 nm, [8]. Depth & height is normalized to the range [0, 1] and is relative to an arbitrary zero depth. The low frequency curvature caused by either deformation of the image by extraction from the container, stress release after extraction, or non-horizontal placement on the stage is clearly evident as the color change from lower left to upper right corners.

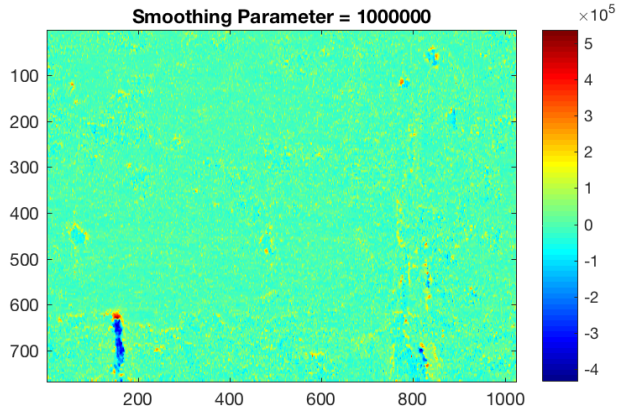

Fig. 6. Example of background removed depth & height data, 768 rows by 1024 columns image, from a confocal microscope ".vk4" data file. Axes represent row (vertical) and column (horizontal) pixel numbers. Pixel width and height are both 690 nm, [8]. The background is removed with the subroutine SMOOTHN [22], [23], [24], in MATLAB version 2017a using a fixed smoothing parameter of 1,000,000. The low frequency curvature of Fig. 5 has been removed. The zero value now represents the mean surface height & depth. Negative values are below the surface and positive values are above the surface. The units are arbitrary microscope units proportional to microns.

Comparison of Fig. 5 with Fig. 6 gives a visual idea of how the low frequency background is removed from the original data while having a minimal effect on the higher frequency features on the surface.

In addition to the optical and depth & height data, the ".vk4" file also contains intensity and laser optical data. Examples of intensity and laser optical data types are portrayed in Figs. 7 and 8. The intensity data has a univariate number for each pixel in the image and is related to the maximal intensity of reflected laser light as measured by the microscope. The laser optical data is an integer triple corresponding to the red, green, and blue color channels for each pixel in the image and is related to the laser intensity and color of the surface as measured by the microscope, [20]. These additional types of data, intensity, optical, and laser optical, do not appear to suffer from the background "tilt" issue that occurs with the depth & height data.

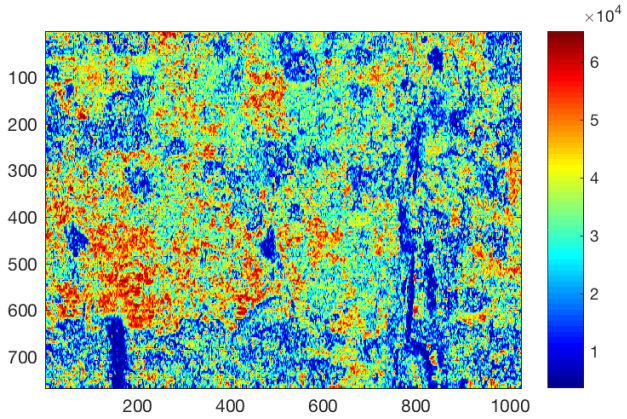

Fig. 7. Example of intensity data, 768 rows by 1024 columns image, from a confocal microscope ".vk4" data file. Axes represent row (vertical) and column (horizontal) pixel numbers. Pixel width and height are both 690 nm, [8]. Intensity is unnormalized in microscope selected output units.

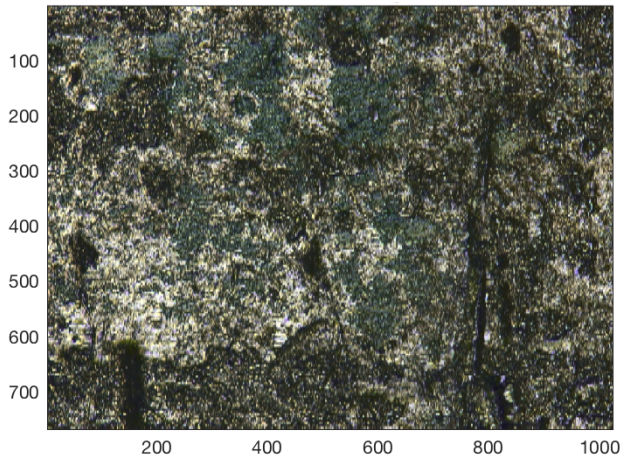

Fig. 8. Example of laser optical data, 768 rows by 1024 columns image, from a confocal microscope ".vk4" data file. Axes represent row (vertical) and column (horizontal) pixel numbers. Pixel width and height are both 690 nm, [8]. Although, coded in color, the image appears rather monochrome or bland, exhibiting a hint of blue-green and light tan colors, along with the grey and black features. Dark oval-like features may be potential pits and elongated dark features may be potential cracks.

The ".vk4" file data consist of 768 by 1024 by 8 channels or data "types". These (8) types are: depth & height (1 integer value), intensity (1 integer value), optical RGB (3 integers in (0,255)), and laser optical RGB (3 integers in (0,255)). Contact [20] or see [19] for more data detail. It is anticipated that there will be approximately 6,000 images for one inspected inner 3013 container. These images are taken around the circumference of the container near the weld where internal stress is maximal. This will result in 768 x1024 x 8 x 6,000 = 37,748,736,000 data values or numbers, for the image data of one container. Accurate human inspection of this amount of data is impractical or impossible. Human inspection of this quantity of data requires some sort of automation. It is proposed here that a system may be devised that identifies images that require further human inspection, may require further human inspection and those that do not require further human inspection. For simplicity we label these red, yellow, and green flagged images, respectively.

B. Stringer Data

The photographic image in Fig. 2 is from the cross section of the lid of a SAVY container, [9]. A sample of three sections of the cross section were analyzed in [9]. The stringer's are very small channels in the container lid that may traverse the entire lid material possibly allowing for minute gas release. The tell-tail sign of the stringer are the dark spots and lines on the cross section of the lid which have been determined to be MnS. The SAVY specifications require that the sulfur content of the lid material be less than a specific amount. Once the ratio of MnS area to the lid cross section area is known the sulfur content may be estimated. The three estimates, one from each sample, may be combined and applied to the entire lid cross section area to determine an estimate of the lid sulfur content in the plane of the cross section. This amount may be further extrapolated to the entire lid volume resulting in an estimate of the lid sulfur content. The analysis described here is to demonstrate the ability to determine this ratio from the photographic image, Fig. 2.

III. Analysis and Discovery Outline

A. LCM Analysis and Discovery

After the background is removed from the raw data one may see features above and below the background as in Fig. 6. In this figure there are features both above and below the surface. In theory the microscope measures the height with additive unbiased noise. Visually, this microscope related noise is quite considerable making it hard to discern some features when looking at and rotating the data in a 3-d MATLAB figure, not shown here. The noise has a distribution with standard deviation around 5%. If the standard deviation was equal to zero then the features could be defined or signal known exactly. The standard deviation is not zero and so the definition of features includes a confounding of the signal with the noise. The 5% value is intermediate and allows some shallow but broad features as well as some deep but narrow features to be identified. It is left as future research to determine the precise influence of the magnitude of the standard deviation on the identification of features with various sizes and shapes. The

signal to noise ratio varies with the features in the image. Some features will be swamped by the noise and others will be quite clear in spite of the noise. In addition, it appears from preliminary observations that the noise is not symmetric when encountering the edge of a feature. The effect of this asymmetry is not further studied here.

1) Possible Surface Features: There are many apparent features on the images portrayed in Figs. 6, 7, 1, and 8. For depth & height and intensity data, possible image features of interest are determined by thresholding the image values and then determining neighborhoods of pixels that passed the threshold test. In a similar way, for optical and laser optical data the thresholding is done by determining values of red, green, and blue coordinates that fall within a desired RGB space volume. This volume is defined by a polytope in RGB space, see [25] and [26]. Fig. 9 is a scatterplot for the laser intensity data of another corrosion sample ".vk4" data file from a 3013 container HCL test example, see [25]. Each pixel in Fig. 9 is plotted at its corresponding RGB values in 3-space and is colored according to whether or not the RGB triple falls within a user defined polytope. In this case the polytope is a user defined cube. The pixels that fall within the polytope, colored red in the figure, are used for feature creation as described in [21], [25], and [26].

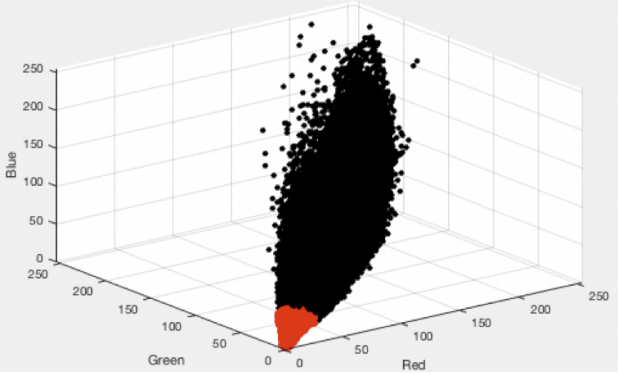

Fig. 9. Laser optical pixel red, green, and blue image values are plotted in RGB space as black or red circles. Red circles indicate the pixels are used to create the features [25]. Black circles are for pixel data that is not used in the feature creation. Data is from an experimental corrosion ".vk4" data file from a 3013 container HCL test example, see [25]

An example feature from height data of a ".vk4" file, [21], is provided in Fig. 10. It can be seen that the feature is contiguous, including corners of the pixels, and may or may not contain voids. The features may be rather complex as seen in Fig. 10.

2) Statistics Related to Possible Surface Features: A group of neighboring pixels determines a possible feature, [21]. Statistics are computed for each of the possible surface features from each of the data types. The possible features are uniquely labeled and related statistics include:

1) Data type origin (type of data used to define feature, ie. height)
2) Pixel locations (row and column locations of the pixels in the image)

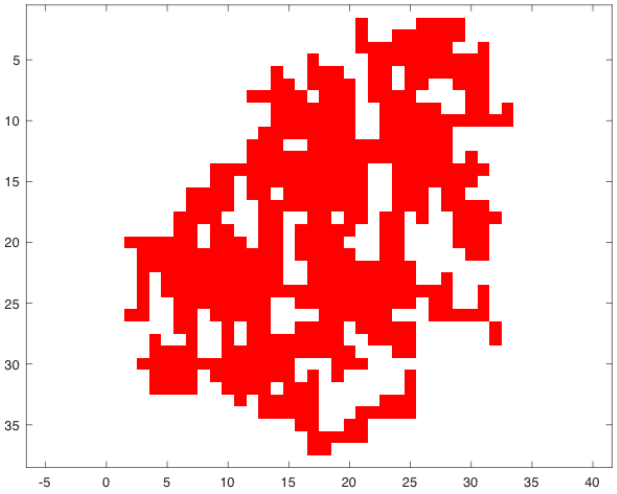

Fig. 10. Example feature with one hole identified by Euler number. [21].

3) Number of pixels or area in square microns (area of the feature, number or square microns)
4) Orientation (angle of the major axis of the feature, defined in MATLAB)
5) Eccentricity (defined in MATLAB)
6) Centroid (defined in MATLAB)
7) Bounding box (defined in MATLAB)
8) Euler number (defined in MATLAB)
9) Convex Area (defined in MATLAB)
10) Equivalent Diameter (defined in MATLAB)
11) Solidity (defined in MATLAB)
12) Extent (defined in MATLAB)
13) Perimeter (defined in MATLAB)
14) Number of pixels (defined in MATLAB)
15) Pixel length in nano-meters (length of square side of a pixel)
16) Below and above surface areas (area above the smooth level of the height surface)
17) Maximum depth or height (the deepest or highest pixel in a height feature)
18) Below and above surface variability - roughness (the standard deviation of the height of the pixels in a feature)
19) Below and above surface volume (sum of depth & height times pixel area)
20) Below and above surface average depth or height (the average of the below or above height of the pixels in a feature)

3) Classification of Possible Surface Features: The possible surface feature statistics are used to classify each of the possible features as of concern or not of concern. The classification categories are: pit-like and crack-like.

The pit-like category requires the feature to be of at least a certain area and of at least a certain maximum depth. The exact cutoff values for area and depth are being developed as those that create a feature of concern, possibly of concern, or not of concern to a subject matter expert, see [21], for specific values used.

The crack-like category requires the feature to be of at least a certain area and of at least a certain eccentricity. The exact cutoff values for area and eccentricity are being developed as those that make the feature of concern, possibly of concern or not of concern to a subject matter expert, see [21], for specific values used.

The use of all of the feature statistics described above, to determine the features of interest, is being pursued as continued research. Currently, it has been found that maximum depth is very useful for potential pit detection and the eccentricity is very useful for potential crack detection. In addition, number of pixels has been useful for detection of both potential pits and potential cracks. A feature is flagged as red, yellow, or green based upon these feature classifications.

In the quantification of MnS the statistics of interest are the area the features and optical data type origin forming the features. A feature is flagged as MnS based upon these feature classifications.

In the methodology described here, and with further continued research, the use of the feature statistics allow for the classification of features to accomplish the specific visualization and research goals.

4) Classification of Images by Classification of Surface Features: Individual images may now be classified as of concern or not of concern based upon whether or not it contains red or yellow flagged features. To determine a flagged feature one needs to consider the following possible features.

1) Identify a pit - What is a pit?
2) Identify maximum depth of a pit - Over what area?
3) Identify a crack - What is a crack?
4) General Corrosion
5) Machining marks
6) Scratches
7) Polishing marks
8) Voids

This methodology is intended to provide statistics that help to determine the type of feature on the material surface. A potential crack feature is not simple a blemish on the surface but rather something very specific and must be corroborated by a material science subject matter expert. An additional study, specifically incorporating the subject matter information about corrosion, including cracks, is under development and will be described elsewhere.

B. Stringer Analysis and Discovery

The stringer analysis proceeded in a similar way as the LCM analysis of the optical and laser optical data. The stringer data consists of red, green, and blue channels for the images. To quantify the image features of interest one proceeds as:

1) Read image data into a matrix
2) Determine the RGB polytope of dark pixel values
3) Determine the area of the entire image canvas (minus the length key inset)
4) Export the stringer area and total area

The polytope selection is a subjective determination of the polytope based upon the features identified. The features identified in Fig. 2 are portrayed in Fig. 11 using the cutoff value, 150, from [9]. Fig. 12 shows the red, green, and blue values for the image as black or red circles. Red circles indicate the RGB pixel values for pixels used to create the features. Black circles represent the RGB pixel values for pixels not in a feature. The polytope methodology in Fig. 12 is the same as that mentioned earlier in Fig. 9.

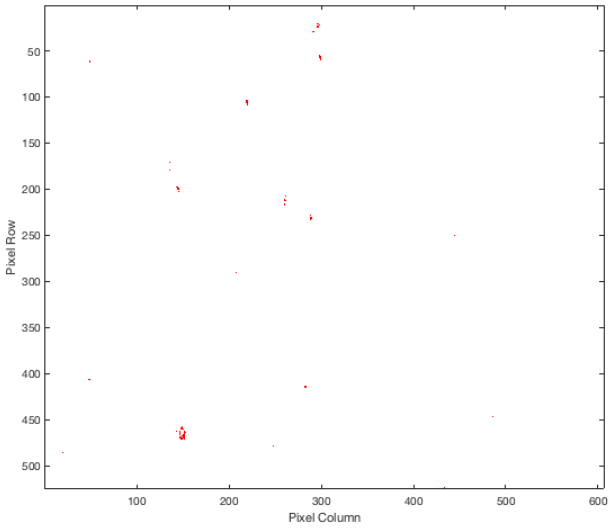

Fig. 11. Stringer features in red corresponding to Fig. 2 from [9].

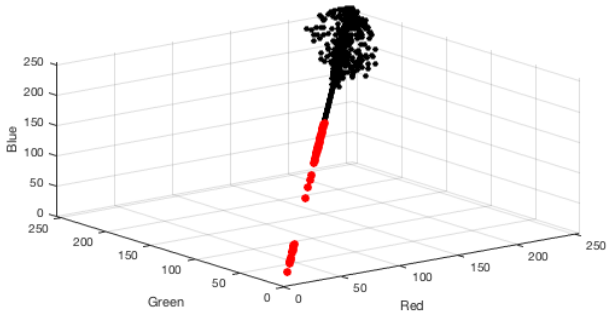

Fig. 12. Stringer pixel red, green, and blue image values are plotted in RGB space as black or red circles. Red circles indicate the pixels are used to create the features [9]. Black circles are for pixel data that is not used in the feature creation.

A study of Fig. 11 revealed single pixel features that did not appear to be different from simple additive noise rather than single pixel signal. It was decided to remove this source of "noise" from the image by removing these single pixel features from further analysis. They are not used in the determination of the amount of MnS in the image. Excluding features in Fig. 11 with exactly one pixel in the feature results in Fig. 13. Only a few features are removed by this process. Excluding features in Fig. 11 with exactly one or exactly two pixels in a feature results in Fig. 14. A few more features are removed by this process. The precise number of pixels removed is listed in [9].

Removing three or more pixel features was not desired by the subject matter experts.

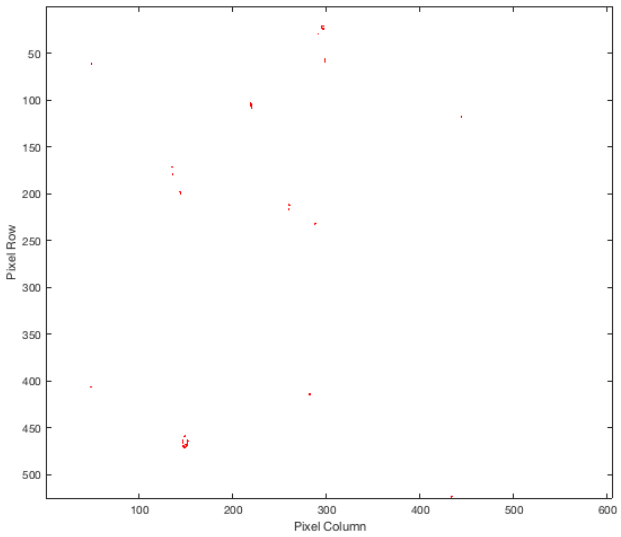

Fig. 13. Stringer features in red, 2 or more pixels in size retained, corresponding to Fig. 2 from [9].

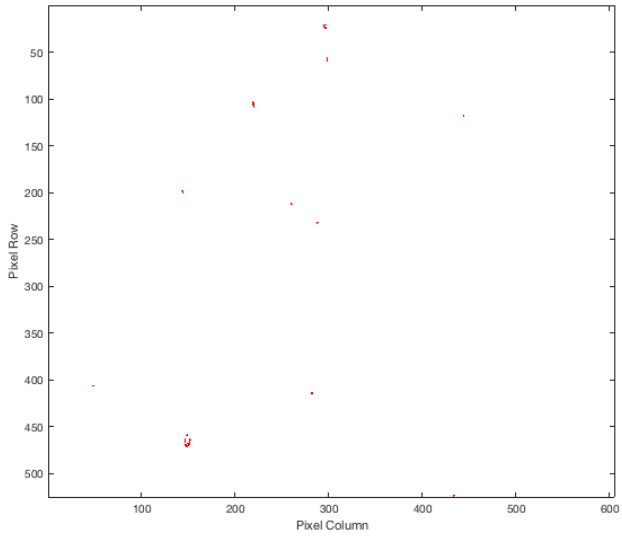

Fig. 14. Stringer features in red, 3 or more pixels in size retained, corresponding to Fig. 2 from [9].

There are three stringer analysis pictures sampled from the lid cross section, one in Fig. 2, and the other two portrayed in Fig. 15 and Fig. 16 zoomed as in Fig. 3 to help make some stringers visible.

The feature creation process for Fig. 15 with only two or more pixel features retained results in the features in Fig. 17.

The feature creation process for Fig. 16 with only two or more pixel features retained results in the features in Fig. 18.

Upon discussion of the feature creation process in [9] with the subject matter experts it was decided to use the statistics from the features with one pixel feature excluded, as in, Figs. 13, 17, and 18. The stringer area ratio for the three stringer images is 0.00034, 0.000894, and 0.00141 for Figs. 13, 17, and 18, respectively. The average, maximum, and minimum sulfur weight percents were estimated at 0.017, 0.027, and 0.006, all

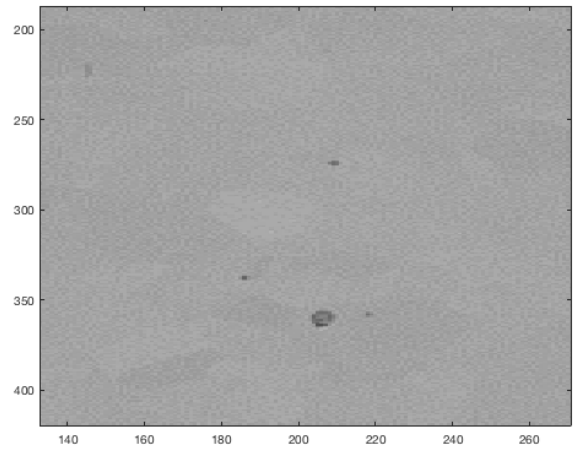

Fig. 15. Second SAVY container zoom in of original (not displayed) photographic image. Dark areas are indicative of stringers containing MnS, [9]. Original image is 525 rows and 608 columns of pixels. Axes values reflect rows and columns of the zoom area.

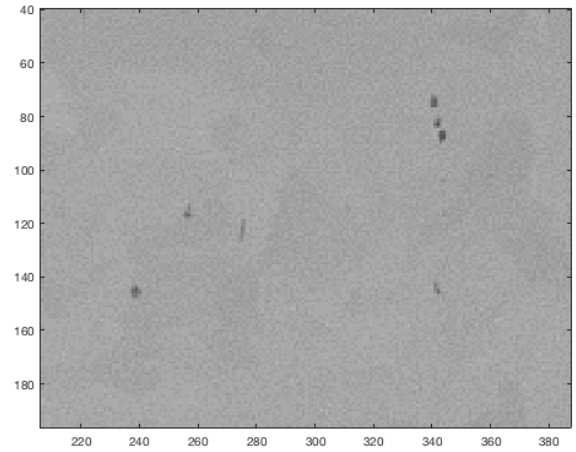

Fig. 16. Third SAVY container zoom in of original (not displayed) photographic image. Dark areas are indicative of stringers containing MnS, [9]. Original image is 525 rows and 608 columns of pixels. Axes values reflect rows and columns of the zoom area.

of which meet the specification of $< 0.03\%$.

IV. Analysis and Discovery Results

The results include the creation of features based upon intensity, optical, and laser optical data. The depth data may then be used with these data types to create new features for characterization. In addition, the methodology used on the LCM optical and laser optical images may be utilized in the stringer analysis. The analysis of the stringer images is discussed and was used as input to determine quantities of MnS in the plane of the cross section of the lid.

The visualization involved in the LCM analysis along with discussions with the subject matter experts evolved the concep-

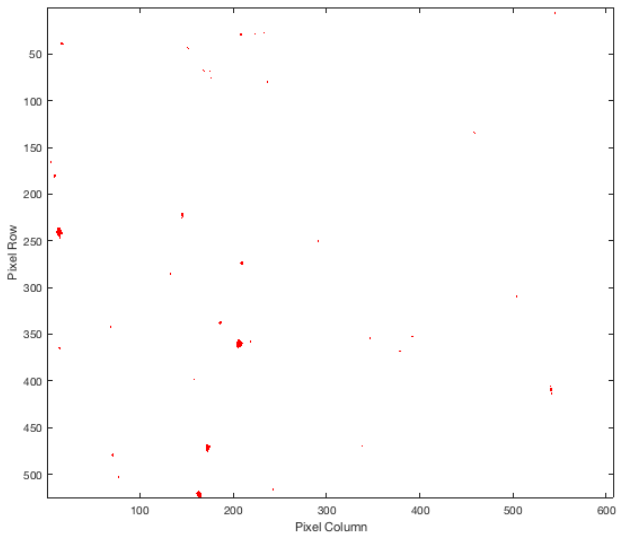

Fig. 17. Second SAVY stringer features, 2 or more pixels in size retained, corresponding to Fig. 15 from [9].

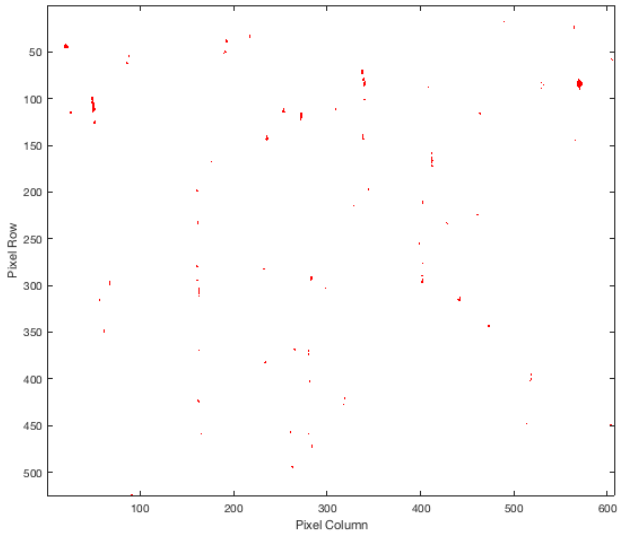

Fig. 18. Third SAVY stringer features in red, 2 or more pixels in size retained, corresponding to Fig. 16 from [9].

tual appearance of a potential crack. This evolution proceeded by thinking of a potential crack as:

1) Linear line segment
2) Linear rectangle
3) Linear Rectangle with depth
4) Curvy feature with depth
5) Curvy feature with varying depths
6) 3-d embedded feature in 3-d sample
7) Completely open to completely closed at the surface
8) May have height or rim build up

The conceptualization of cracks continues to be modified to help drive the analysis of the data. Eventually it is desired to discriminate between actual cracks (stress created) and crack-like (scratches, machining marks, linear voids) features.

V. Visualization

Visualization aspects include the methodology presented above to identify potential pits, potential cracks, and general surface corrosion from container images. This work is currently in progress. We now have approximately 6,000 images from one 3013 container and are in the process of analyzing these images with the automatic corrosion detection methodology. As a precursor to this work we are working with the material science subject matter experts to minimize the errors in identification and to maximize the likelihood of corrosion detection when it exists. When corrosion exists do we detect it or not? When corrosion does not exist do we detect any or not? Summarizing this we have detection probabilities and errors probabilities. These are the typical type one and type two errors associated with hypothesis testing. This fine tuning of the parameters in the automatic detection software will be described elsewhere. The parameters themselves are described in [21], [25], and plan to be published in the proceedings of the 2018 Joint Statistical Meetings held in Vancouver, British Columbia, Canada. The visualization parameters are not further described here in much more detail in order to "not substantially overlap work which has been published elsewhere or simultaneously submitted to a journal or another conference with proceedings." We envision the analysis of the 6,000 images to initially be an iterative process where the images are categorized by the methodology, the subject matter experts evaluate the categorization results, the methodology is improved, and this process repeated until the methodology performs well on additional container images as evaluated by the experts.

VI. Future Work

The ultimate goal of this work is automation on the LCM data and efficient use on non-LCM data. The methodology for doing this is outlined above, it remains to acquire additional data, and implement the methodology.

Potential cracks identified here may be part of a larger crack or crack system. Joining together of individual potential features to create features representing the larger crack or crack systems is desirable. In a similar way, smaller features may be aggregated to represent and identify surface stress corrosion areas.

Actual stress cracks have been identified and are being used to help characterize a feature as requiring further scrutiny or not.

There are multiple additional applications that have been identified for this visualization and discovery analysis. These include an example of lithium battery images, [27], corrosion over time, and evaluating LCM images of aluminum coupons as an indicator of the degradation of the aluminum-clad spent nuclear fuel[1].

[1]Personal Communication with Elizabeth Kelly of Los Alamos National Laboratory.

ACKNOWLEDGMENT

Juan Duque and Michael Martinez-Rodriguez provided the microscope ".vk4" file data utilized in the development of the software. Collaboration with John Berg, Juan Duque, Jonathan Gigax, Tristan Karns, Kimberly Kaufeld, Elizabeth Kelly, Michael Martinez-Rodriguez, and Raj Vaidya improved the methodologies employed.

REFERENCES

[1] P. H. Smith, "Plutonium Packaging," Los Alamos National Laboratory Report, LA-UR-17-24871.

[2] K. P. Reeves, T. Karns, E. Weis, J. M. Oka, P. H. Smith, T. A. Stone, and J. E. Narlesky, "Surveillance Report on SAVY-4000 and Hagan Nuclear Material Storage Containers for FY 2017," Los Alamos National Laboratory Report, LA-UR-17-31263.

[3] DOE-STD-3013-2012, "Stabilization, Packaging, and Storage of Plutonium-Bearing Materials," DOE-STD-3013-2012, U.S. Department of Energy, Washington, D.C., 20585, United States of America, pp. i-viii, and 1–75, March 2012.

[4] ASTM A479/479M-18, "Standard Specification for Stainless Steel Bars and Shapes for Use in Boilers and other Pressure Vessels," https://www.astm.org/Standards/A479.

[5] P. H. Smith, T. Karns, T. A. Stone, J. G. Teague, D. K. Veirs, N. Guadagnoli, C. Marks, L. Anderson, and R. Clark, "Testing and Versatility of the SAVY 4000 Nuclear Material Container 15634," Los Alamos National Laboratory Report, LA-UR-14-29021.

[6] P. H. Smith, T. A. Stone, T. Karns, K. P. Reeves, J. M. Oka, T. F. Yarbro, R. J. C. Bachman, E. Weis, M. W. Blair, and D. K. Veirs, "The SAVY 4000 Container Storage Program at Los Alamos National Laboratory," Los Alamos National Laboratory Presentation Report, LA-UR-16-25367.

[7] P. H. Smith, T. A. Stone, T. Karns, K. P. Reeves, J. M. Oka, T. F. Yarbro, R. J. C. Bachman, E. Weis, M. W. Blair, and D. K. Veirs, "The SAVY 4000 Container Storage Program at Los Alamos National Laboratory," Los Alamos National Laboratory Report, LA-UR-16-24023.

[8] J. G. Wendelberger, "Container Surface Evaluation by Function Estimation," Los Alamos National Laboratory Report, LA-UR-17-26844.

[9] J. G. Wendelberger, "Image Analysis of Stringer Area: Three Images," Los Alamos National Laboratory Report, LA-UR-18-27762.

[10] J. K. Dienes "On the mean cluster size of a network of cracks," in Structural Control and Health Monitoring: The Official Journal of the International Association for Structural Control and Monitoring and of the European Association for the Control of Structures, vol. 13, no. 1, pp. 169–189, 2006.

[11] Q. H. Zuo, J. K. Dienes, J. Middleditch, and H. W. Meyer Jr., "Modeling anisotropic damage in an encapsulated ceramic under ballistic impact," in Journal of Applied Physics, vol. 104, 023508, pp. 1-10, 2008.

[12] A. Dean, S. Sahraee, K. zenc, J. Reinoso, R. Rolfes, and M. Kaliske, "A thermodynamically consistent framework to couple damage and plasticity microplane-based formulations for fracture modeling: development and algorithmic treatment," in International Journal of Fracture, Vol. 203, Issue 1-2, pp. 115-134, January 2017.

[13] D. Marn, A. Aquino, M. E. Gegndez-Arias, and J. Manuel Bravo, "A New Supervised Method for Blood Vessel Segmentation in Retinal Images by Using Gray-Level and Moment Invariants-Based Features," in IEEE Transactions on Medical Imaging, Vol. 30, No. 1, January 2011.

[14] P. Subirats, J. Dumoulin, V. Legeay, and D. Barba,"Automation of Pavement Surface Crack Detection using the Continuous Wavelet Transform," 2006 International Conference on Image Processing, pp. 3037-3040, 2006.

[15] Q. H. Zuo, L. E. Deganis, and G. Wang, "Elastic waves and damage quantification in brittle material with evolving damage," J. Phys. D: Appl. Phys. 45, 145302 (8pp), 2012.

[16] A. B. Kunin, and Q. H. Zuo, "Stability and well-posedness of a rate-dependent damage model for brittle materials based on crack mechanics," Applied Mathematical Modelling, Vol. 40, pp. 38013811, 2016.

[17] I. A. Ovid'ko, and A. G. Sheinerman, "Nanoscale cracks at deformation twins stopped by grain boundaries in bulk and thin-film materials with nanocrystalline and ultrafine-grained structures," J. Phys. D: Appl. Phys., Vol. 47, 015307, 2014.

[18] E. Kelly, "A General Statistical Model for Corrosion Pit Depth Analysis for Threshold Data," Los Alamos National Laboratory Report, LA-UR-13-27205.

[19] J. G. Wendelberger, "Reading a vk4 File, Utilizing Polytopes for Multivariate RGB Images," Los Alamos National Laboratory Report, LA-UR-18-28722.

[20] Keyence Corporation of America, 500 Park Boulevard, Suite 200, Itasca, IL 60143, United States of America.

[21] J. G. Wendelberger, J. Duque, E. J. Kelly, J. M. Berg, and K. A. Kaufeld, "Container Surface Evaluation: Background Estimation, Background Removal, Feature Detection, and Image Ranking," Los Alamos National Laboratory Report, LA-UR-17-28052.

[22] D. Garcia, "Robust smoothing of gridded data in one and higher dimensions with missing values," Computational Statistics and Data Analysis, Vol. 54,1167-1178, 2010.

[23] D. Garcia, "A fast all-in-one method for automated post-processing of PIV data," Exp Fluids, Vol. 50, pp. 12471259, 2011.

[24] Garcia, D., Fast 'n easy smoothing, SMOOTHN, Version 2.1.1, https://www.mathworks.com/matlabcentral/fileexchange/25634-fast–n-easy-smoothing?s_tid=prof_contriblnk, 25 July 2016.

[25] J. G. Wendelberger, "The Identification and Quantification of Pits, Cracks, and Corrosion from Container Material Image Surface Depth Measurements with Subsequent Container Classification," Los Alamos National Laboratory Report, LA-UR-18-26193.

[26] S. Mutha, S. Dorta, I. A. Sebagb, M. Blaisb, and D. Garcia, "Unsupervised dealiasing and denoising of color-Doppler data," Medical Image Analysis, Vol. 15, Issue 4, Pages 577-588, August 2011.

[27] B. L. Mehdi, J. Qian, E. Nasybulin, C. Park, D. A. Welch, R. Faller, H. Mehta, W. A. Henderson, W. Xu, C. M. Wang, J. E. Evans, J. Liu, J. -G. Zhang, K. T. Mueller, and N. D. Browning, "Observation and Quantification of Nanoscale Processes in Lithium Batteries by Operando Electrochemical (S)TEM," Nano Letters 2015 15 (3), 2168-2173, DOI: 10.1021/acs.nanolett.5b00175.